

Available online at www.sciencedirect.com**SciVerse ScienceDirect**

Procedia Engineering 19 (2011) 73 – 80

**Procedia
Engineering**www.elsevier.com/locate/procedia1st CIRP Conference on Surface Integrity (CSI)

A model of material removal and post process surface topography for copper CMP

S. Choi^{a*}, F. M. Doyle^b, D. Dornfeld^a^aUniversity of California, Berkeley, Department of Mechanical Engineering, Berkeley, California 94720-1740, USA^bUniversity of California, Berkeley, Department of Materials Science and Engineering, Berkeley, California 94720-1760, USA

Abstract

Increasing systemic error during copper CMP (Chemical Mechanical Planarization) is due to the uneven surface topography generated during the process. A mechanistic model based on a fundamental understanding of the process constituents was proposed to predict material removal rates and the post CMP topography. Two synergistic mechanisms were proposed: 1) chemically dominant behavior is explained by the repetitive removal and formation of a protective layer on copper surface and chemical dissolution during the process, 2) mechanically dominant removal mechanism is due to the material behavior of copper at the nano-scale and subsequent oxidation and removal of the plastically deformed copper. As a step forward to optimize the process and the manufacturing system, this model was extended to explain pattern dependent variability during copper CMP.

© 2012 Published by Elsevier Ltd. Open access under [CC BY-NC-ND license](#).

Selection and peer-review under responsibility of Prof. E. Brinksmeier

Keywords: Semiconductor, Modelling, CMP

1. Introduction

Copper CMP (Chemical Mechanical Planarization) is a technique used to planarize uneven wafer surfaces during semiconductor manufacturing processes. It has been a key enabling technology for copper multilevel metallization of semiconductor interconnects. With scaling down of the semiconductor devices and interconnects, and enlargement of the wafer size, the process requirements for copper CMP have become more challenging (i.e. requiring less variation in height (step height) of the polished surface and less defect level, etc) [1]. Moreover, major yield loss during manufacturing of the semiconductor devices

* Corresponding author. Tel.: 5105296547

E-mail address: choisch@berkeley.edu

is increasingly related to the design of the chips (i.e. systemic errors) rather than to the processes (i.e. random errors) as the devices are scaled down. Design for Manufacturability (DfM) has been adopted to address this systemic error of the manufacturing system. However, currently available DfM tools utilize an empirical process model (based on Preston's equation [2]) of copper CMP, requiring a significant amount of calibration through experiment. Therefore, a new CMP model that reduces the burden of the calibration is required.

Although many CMP models have been developed by different researchers [2-5], most of them were insufficient at explaining the material removal mechanism during copper CMP. A synergistic model was proposed by Tripathi *et al.* for copper CMP [6]. They assumed that the passivation layer formed is thick enough that the abrasives or pad asperities remove only some fraction of the passivation layer at the top. They also neglected the direct removal of copper by the action of abrasives or asperities. However, it is evident from experimental data [7-9] that mechanical action alone (without any chemicals) can remove some copper. Also, the time between consecutive asperity and copper interactions is too short for forming a thick layer of the protective (passivation) material. Therefore, both mechanical and chemical aspects and their synergism must be considered to account for the material removal mechanism during copper CMP. In this study, a quantitative and mechanistic model of copper CMP that predicts MRR is proposed and extended to explain pattern dependent variability during the process.

Nomenclature

A_{as}	average contact area between an asperity and copper
A_c	cross-sectional area of a trench generated by abrasives
A_w	surface area of wafer
$Ar\%$	real contact area ratio
F	Faraday's constant
K_1	correction factor accounting for partial removal of oxidized pile up copper
K_2	correction factor accounting for material removal only on or at vicinity of grain boundaries.
M_{Cu}	atomic mass of copper
n	oxidation state of the oxidized copper
N_{ab}	number of abrasives trapped by asperities
t_{as}	interval between consecutive an asperity and copper contacts
v	sliding velocity of abrasives
ρ	density of copper

2. Modeling of Copper CMP to Predict MRR

A quantitative and mechanistic model for copper CMP is proposed partly based on the model by Tripathi *et al.* [6]. To overcome the limitation of the previous models, a wide range of input parameters are considered and the synergism between chemical and mechanical aspects is considered. The model can

be illustrated as follows: A fraction of the copper surface is occupied by protective material formed by slurry chemistry. During the interaction of copper and a CMP pad asperity/abrasives a fraction of the protective material is removed, then reformed before the next asperity/abrasives interaction. During the time period between consecutive asperity and copper interactions, active chemical dissolution of copper occurs at both protected and unprotected sites, but with different rates. The removal of copper by the dissolution and by the protective material removal is termed chemically dominant material removal. In addition, the force applied by abrasives trapped between pad asperities and copper will cause plastic deformation of the copper if the shear stress induced by the abrasives overcomes the shear strength of copper. This deformation is restricted to the region where defects in the crystal structure are accumulated (such as at grain boundaries). Deformed material will be piled up along the trenches created by the sliding path of the abrasives, then successively oxidized and removed by subsequent asperities/abrasives interactions. This type of material removal is termed mechanically dominant material removal. The overall MRR during copper CMP (MRR_{total}) is estimated by adding these chemically (MRR_{chem}) and mechanically dominant (MRR_{mech}) components.

2.1. Chemically Dominant Material Removal Mechanism

The chemically dominant mechanism can be explained using Figure 1. Once the force exerted on copper by pad asperities is determined (Figure 1(a)), the fraction of the protective material that is removed during the interaction of an asperity and copper can be estimated (Figure 1(b)). This is defined as the removal efficiency (η). The frequency of asperity/copper interactions and the removal efficiency determine the characteristic time t_0 which dictates how much area of copper is occupied by the protective material, which is termed as coverage ratio, θ (Figure 1(c)). The coverage ratio right after the interaction by an asperity is the value at t_0 and right before the next interaction by an asperity is the value at t_0+t_{as} . During copper CMP the coverage ratio changes cyclically between these two values and the amount of copper oxidized (by dissolution and by forming the protective material) can be calculated by evaluating the area under the current density curve between t_0 and t_0+t_{as} . Thus, the chemically dominant removal of copper can be calculated using Faraday's law as shown in equation (1). Those three components of this mechanism are explained as follows.

$$MRR_{chem} = \frac{M_{Cu}}{\rho n F \tau} \int_{t_0}^{t_0+t_{as}} i(t) dt \quad (1)$$

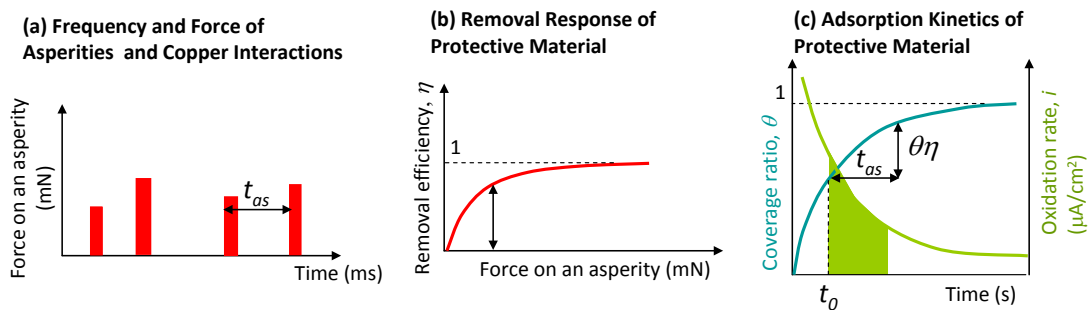


Figure 1. Modeling framework for the chemically dominant material removal mechanism

The frequency of asperity/copper interactions can be determined by evaluating the real contact area ratio and the average area of each contact. Those data were obtained from optical images of the contact interface [10]. Based on the data, the interval between consecutive asperity/copper contacts was determined to be 1-10 ms and the duration of each contact was 10 μ s.

The relationship between the removal efficiency and the force applied on copper by an asperity was determined by comparing the area swept by an asperity and the area swept by the abrasives trapped between the asperity and copper during the interaction of an asperity and copper. It was assumed that the sweeping action of abrasives embedded in an asperity generates linear trenches on the copper surface. The determined relationship between the removal efficiency and the number of trapped abrasives for typical CMP condition is shown in Figure 2(a). The contact area between an asperity and copper was assumed to 100 μ m² and the abrasive sizes were 100 nm in diameter.

The adsorption kinetics of the protective material on copper in pH 4 aqueous solution containing 0.01M BTA and 0.01M glycine were theoretically analyzed [11], supplying direct input to the model. The chemically dominant material removal rate during copper CMP can be determined by considering all of these inputs.

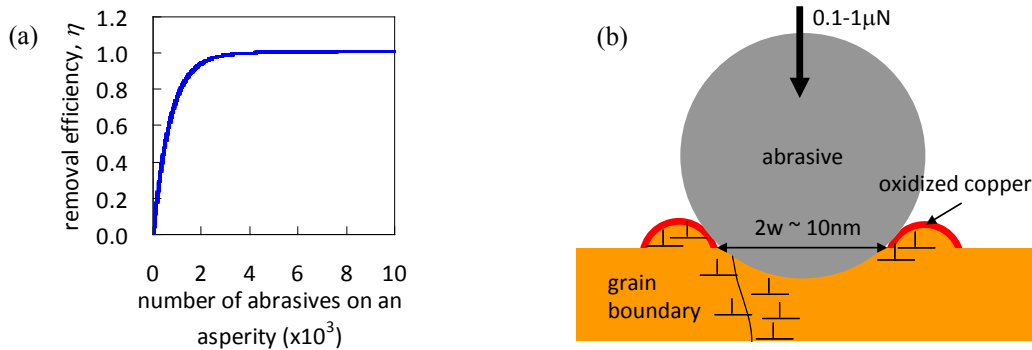


Figure 2. (a) Dependence of the removal efficiency on the number of abrasives trapped in between an asperity and copper; (b) Indentation of an abrasive into copper at the nano-scale during copper CMP

2.2. Mechanically Dominant Material Removal Mechanism

Previous analysis of the mechanical response to the force applied by abrasives to copper was based on mechanical material properties obtained at the macro-scale [3]. The predicted MRR [3] was three orders of magnitude higher than the experimental values [7-9], suggesting the need for a new approach. Figure 2(b) shows the interaction of an abrasive and copper during copper CMP. The force exerted on copper by an abrasive was evaluated to be 0.1-1 μ N for typical copper CMP process. Since the size of grains of copper (about 1 μ m in diameter) is much larger than the contact area by an abrasive (about 10 nm in diameter), the plastic deformation of copper should be induced by homogeneous nucleation of the dislocations in the crystal of copper. Therefore, nano-scale material behavior is highly relevant to this case. The resolved shear strength of copper by nano-indentation on the inside of the grain was 10.6 GPa [12], which is nearly three orders of magnitude larger than the value at the macro-scale (42 MPa). This value is in fact much larger than the shear stress induced by the abrasives during copper CMP, 1.4-2.9

GPa (estimated by assuming 1000 abrasive particles of 100 nm diameter are trapped in $100 \mu\text{m}^2$ of contact area between copper and an asperity), implying that the deformation of copper is elastic when an abrasive interacts at the inside of a copper grain. Therefore, it is suggested that plastic deformation only occurs at sites with high concentrations of defects, such as the grain boundaries and the vicinity of plastically deformed regions. Once the copper is plastically deformed, copper will be piled up along the trench formed by the indentation (Figure 2(b)). The surface of the piled up material will be preferentially oxidized by the oxidant and dissolved oxygen in the slurry because of the high density of defects and the large surface area to volume ratio. The oxidized copper will be more brittle than the pure copper; and thus the oxidized layer will be removed by subsequent interactions of asperities or abrasives. Therefore, the mechanically dominant removal rate can be calculated as follows:

$$MRR_{mech} = K_1 K_2 \frac{N_{ab} A_c v}{A_w} \quad (2)$$

2.3. Predictions of the Proposed Model

The material removal rate of a 4" copper wafer in a pH 4 slurry containing 0.01 M BTA, 0.01 M glycine and 5 wt% alumina abrasives (100 nm diameter) where potential of copper was controlled to 0.6 V (vs. SCE) by external voltage was estimated to validate the proposed analysis. Here we assume that the average area of contact between the copper and an asperity is independent of the applied pressure, but that the number of asperities that contact the copper increases with increasing pressure. Thus the time between consecutive asperity-copper interactions at a given site is inversely proportional to the real contact area ratio and the sliding velocity:

$$t_{as} = \frac{\sqrt{A_{as}}}{v \cdot Ar\%} \quad (3)$$

The real contact area ratio $Ar\%$ is a linear function of the applied pressure because it captures the number of asperities contacting the copper along with their area [10]. Hence, the time between consecutive asperity-copper interactions is inversely proportional to the applied pressure. Note that with a fixed average area of contact between a given asperity and copper, the number of abrasives embedded in a given asperity and the force transmitted to a single abrasive particle are independent of pressure unless the concentration of abrasives changes. Thus, neglecting any influence of pressure on sliding velocity one would expect the efficiency of a given asperity in removing copper or protective material to be independent of pressure. Finally, when evaluating the force applied to an abrasive particle, it was assumed that only the abrasive particles embedded between an asperity and copper transmit the force applied by the asperity (i.e. the asperity itself does not deform enough by supporting abrasives to contact the surface of copper).

The chemically dominant material removal rate of copper was estimated using equation (1) for current densities measured experimentally in our previous work using glycine solutions containing BTA and externally controlled potentials to induce oxidation [11]. Copper was assumed to oxidize to the Cu^{2+} oxidation state. t_0 was determined from the kinetics of adsorption of BTA and equation (3). The estimated chemically dominant removal rate of copper in this environment is shown in Figure 3. The mechanically dominant removal rate of copper, estimated using equation (2) for the same conditions is also shown in Figure 3. Three different values of the fraction of copper surface undergoing plastic deformation by the

abrasives (K1), namely 0.05%, 0.1% and 0.2%, were assumed. It was also assumed that all the deformed copper forms ridges that are readily oxidized, then removed by subsequent abrasives (see Figure 2(b)). The total removal rate of copper during CMP under these conditions shows that the material removal behavior does follow Preston's equation, supporting the proposed analysis. Also, the magnitude of the MRR is on the order of that observed during conventional copper CMP.

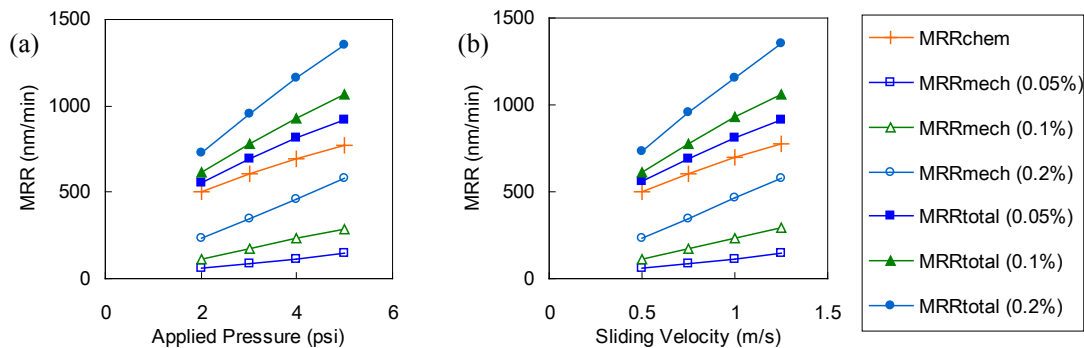


Figure 3. Estimated material removal rates of copper in a pH4 slurry containing 0.01 M BTA, 0.01 M glycine and 5 wt% alumina abrasives (100 nm diameter) where potential of copper was controlled to 0.6 V (vs. SCE) by external voltage: (a) influence of the applied pressure (sliding velocity was 1 m/s) and (b) sliding velocity (applied pressure was 4 psi) showing the influence of different K_I values (0.05%, 0.1% and 0.2%).

3. Modeling to Explain Pattern Dependent Variability

Utilizing the proposed mechanistic CMP model, a modelling framework for the pattern dependent variability is proposed as shown in Figure 4. The success of this approach is dependent on the evaluation of the input parameters to the proposed MRR model. The influence of the wafer topography on the input parameters was qualitatively investigated. Assuming that the length and size of the pad asperities follow a probability distribution function (such as Gaussian distribution), only asperities smaller and longer than the size of a trench can reach the bottom of the trench. In addition, large asperities can deform to reach the bottom of a smaller trench. These two mechanisms affect the number and size of the asperity and copper contact, ultimately influencing the time between consecutive asperity/copper interactions, the removal efficiency and the mechanically dominant removal of copper. As the metal line width increases, the number of asperities that can reach inside of the metal line increases, resulting in decreased time interval between consecutive copper/asperity interactions. This frequent interaction will remove more protective material on the copper surface, allowing more copper to be dissolved. Also, more copper will be deformed and subsequently oxidized by the frequent abrasion by abrasives trapped by the asperities. The expected output is more dishing for wider metal lines as experimentally confirmed [13]. Also, the fact that the grain size of copper is smaller at narrow features on the wafer than at the wider features [14] suggests that copper at narrow lines will be more susceptible to mechanically dominant removal, resulting in dishing. Once the input parameters of the proposed MRR model are evaluated by considering these effects, the local MRR and thus eventually the post CMP topography can be determined if the MRR of dielectrics and barrier materials are known.

4. Conclusion

A quantitative and mechanistic model of copper CMP was proposed considering the synergism between chemical and mechanical aspects of the process. The proposed MRR model was extended to explain pattern dependent variability by considering the influence of the topography on the input parameters of the MRR model. This model qualitatively explains well the dishing behavior during copper CMP. Formulation and experimental validation of the model will be conducted.

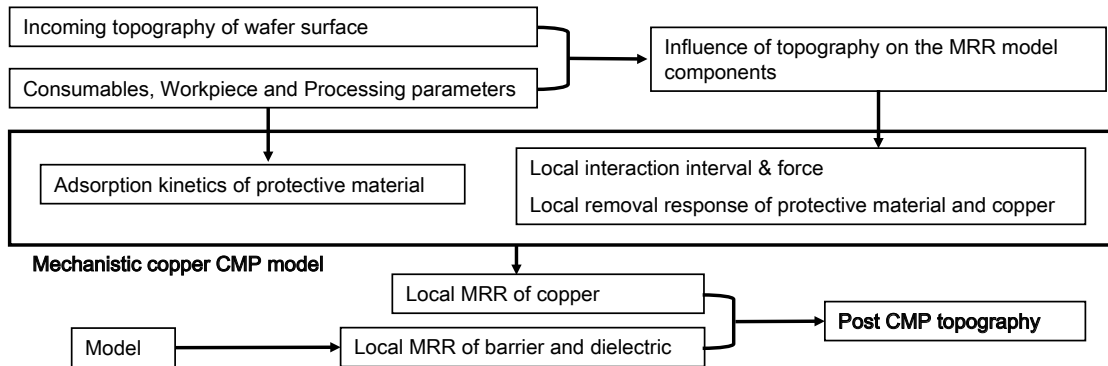


Figure 4. Modeling framework for pattern dependent variability during copper CMP

Acknowledgements

This work was supported in part by the UC Discovery Grant ele07-10283 under the IMPACT program, and AMD, Applied Materials, ASML, Cadence, Canon, Ebara, Hitachi, IBM, Intel, KLA-Tencor, Magma, Marvell, Mentor Graphics, Novellus, Panoramic, SanDisk, Spansion, Synopsys, Tokyo Electron Limited, and Xilinx, with donations from Photonics and Toppan.

References

- [1] *International Technology Roadmap for Semiconductors (ITRS) 2009 Edition*: <http://www.itrs.net/Links/2009ITRS/Home2009.htm>
- [2] Preston FW. The theory and design of plate glass polishing machines. *J. Soc. Glass Technol.* 1927; **11**: 214-56.
- [3] Luo J, Dornfeld DA. Material removal regions in Chemical Mechanical Planarization for Submicron Integrated Circuit Fabrication: Coupling Effects of Slurry Chemicals, Abrasive Size Distribution and Wafer-pad Contact Area. *IEEE Trans. Semicond. Manuf.* 2003; **16**: 45-56.
- [4] Cook LM. Chemical processes in glass polishing. *J. Non-Cryst. Solids* 1990; **120**: 152-71.
- [5] Kaufman FB, Thompson DB, Broadie RE, Jaso MA, Guthrie WL, Pearson DJ et al.. Chemical-Mechanical Polishing for Fabricating Patterned W Metal Features as Chip Interconnects. *Electrochem. Soc.* 1991; **138**: 3460-5.
- [6] Tripathi S, Choi S, Doyle FM, Dornfeld DA. Fundamental Mechanisms of Copper CMP - Passivation Kinetics of Copper in CMP Slurry Constituents. *Mater. Res. Soc. Symp. Proc.* 2009; **1157**, E02-7.
- [7] Chen KW, Wang YL. Study of Non-Preston Phenomena Induced from the Passivated Additives in Copper CMP. *J. Electrochem. Sci.* 2007; **154**: H41-7.

- [8] Balakumar S, Haque T, Kumar AS, Rahman M, Kumar R. Wear Phenomena in Abrasive-Free Copper CMP Process. *J. Electrochem. Sci.* 2005; **152**: G867-74.
- [9] Tsai TH, Yen SC. Localized corrosion effects and modifications of acidic and alkaline slurries on copper chemical mechanical polishing. *Appl. Surf. Sci.* 2003; **210**: 190-205.
- [10] Elmufdi CL, Muldowney GP. The Impact of Diamond Conditioning on Surface Contact in CMP Pads. *Mater. Res. Soc. Symp. Proc.* 2007; **991**: C01-02.
- [11] Choi S, Tripathi S, Dornfeld DA, Doyle FM. Copper CMP Modeling: Millisecond Scale Adsorption Kinetics of Benzotriazole (BTA) in Glycine-Containing Solutions at pH 4. *J. Electrochem. Sci.* 2010; **157**: H1153-9.
- [12] Suresh S, Nieh TG, Choi BW. Nano-indentation of copper thin films on silicon substrates. *Scripta Mater.* 1999; **41**: 951-7.
- [13] Park T, Tugbawa T, Boning D. Overview of methods for characterization of pattern dependencies in copper CMP. *Proc. CMP-MIC 2000*: 196-205, Santa Clara, CA.
- [14] Carreau V, Maitrejean S, Verdier M, Brechet Y, Roule A, Toffoli A, Delaye V et al.. Evolution of Cu microstructure and resistivity during thermal treatment of damascene line: Influence of line width and temperature. *Microelectron. Eng.* 2007; **84**: 2723-8.